A Greedy Approach for Sparse Angular Aperture Radar

Raghu G. Raj, Victor C. Chen, and Ronald Lipps
U.S. Naval Research Laboratory, Radar Division,
Washington D.C. 20375

***Abstract*—We present a novel algorithm for radar imaging of point scatterers using a sparse number of spatially separated sensors. Such sparse sensing scenarios are prototypical of many applications wherein a limited number of sensors are distributed over a geographical area; or where environmental and/or systemic constraints enforce a sparse sampling of angular aperture. Our underlying assumption is that the image is sparse with respect to the Gabor basis set. We then introduce the concept of an orbit—viz. the locus of all projections made by a spatial basis—and formulate the radar imaging problem as that of sparsifying the number of orbits that comprise the radon measurements of the source. We demonstrate how our algorithm outperforms FFT-based and Compressive-sensing based reconstruction algorithms for point-scatterer images, describe relevant theoretical performance bounds of our algorithm, and point to future research arising from this work.**

I. INTRODUCTION

The quality of image formation performed by radar imaging systems fundamentally depends upon its ability to form a 'sufficiently wide enough' aperture to capture the underlying information of interest contained in the scene [1]. In traditional Fourier imaging systems, the sensor outputs from several different aspect angles are combined via back-projection methods [1-3]—which in turn depend upon the Fourier slice theorem [4]—to form an image of the scene. The disadvantage of such an approach is that spatially localized sources of energy (such as due to point scatterers) tend to be correlated with a dense number of slices of the Fourier plane and consequently reconstruction from a sparse number of sensors will cause serious degradation in the quality of the image.

This therefore raises a natural question as to whether it possible to reduce the number of required sensors by imaging with respect to non-Fourier bases in which the image admits a sparse representation. In this paper we formulate this problem as that of sparsifying the number of orbits that are induced by the various spatial atoms that comprise the image with respect to various aspect angles. We define an orbit as the locus of all projections of a given atom with respect to the various aspect angles. The problem of image reconstruction therefore is equivalent to finding the sparest number of orbits that accounts for the radon measurements together with an estimation of the parameters of the spatial atoms that comprise an image.

In this paper we employ the Gabor dictionary to model image structure. One reason for this choice is that, as shown in Section 2, the Radon transform of Gabor atoms yields time-domain Gabor atoms from whose measured properties the parameters of the corresponding spatial Gabors can be inferred. Furthermore, Gabors offer flexible structures to model a range of behaviors from sinusoids to impulses which therefore make it amenable to modeling complex image structures. Thereafter we introduce our basic greedy sparse angular aperture (GSAAR) algorithm for sparse aperture radar imaging, describe some of its properties, and demonstrate quantitative performance bounds of a variant of the GSAAR algorithm.

We numerically evaluate the performance of our algorithm in Section 3 by comparison to traditional back-scattering and compressive sensing based approaches for a varying number of scatterers and varying noise-levels. We find that our algorithm consistently outperforms these approaches for even moderate noise levels and any number of scatterers. We conclude in Section 4 with a discussion of future work and extensions to handle more complicated scene structures.

II. SPARSE ANGULAR APERTURE RADAR

A. Preliminaries

In this paper we model the radar scattering process by the Fourier slice theorem wherein the radar returns from a given aspect is modeled by a slice of the 2-D Fourier transform of the image along the corresponding aspect angle [4]. Given this, the exact image reconstruction is given by the inverse radon transform—which is usually approximated by various back-projection algorithms [2]. However under the constraints of sparse-sensing wherein a sparse number of sensors gather projective information, serious degradation of reconstructed image quality can result due to the fact that the image structures that comprise the image, such as point scatterers, typically exhibit strong correlation with respect to a dense number of slices of the Fourier plane.

Therefore, in this paper, we examine an alternative strategy of imaging in non-Fourier bases with respect to which the source image I admits a sparse representation with respect to the sparse basis set $\{\varphi_i\}_{i=1}^{D}$:

$$I = \sum_{i=1}^{D} c_i \varphi_i(x) \quad (1)$$

Supported by NRL Base Program

Report Documentation Page

Form Approved
OMB No. 0704-0188

1. REPORT DATE	2. REPORT TYPE	3. DATES COVERED
MAY 2010		**00-00-2010 to 00-00-2010**

4. TITLE AND SUBTITLE	5a. CONTRACT NUMBER
A Greedy Approach for Sparse Angular Aperture Radar	5b. GRANT NUMBER
	5c. PROGRAM ELEMENT NUMBER
6. AUTHOR(S)	5d. PROJECT NUMBER
	5e. TASK NUMBER
	5f. WORK UNIT NUMBER
7. PERFORMING ORGANIZATION NAME(S) AND ADDRESS(ES) **U.S. Naval Research Laboratory,Radar Division,Washington,DC,20375**	8. PERFORMING ORGANIZATION REPORT NUMBER
9. SPONSORING/MONITORING AGENCY NAME(S) AND ADDRESS(ES)	10. SPONSOR/MONITOR'S ACRONYM(S)
	11. SPONSOR/MONITOR'S REPORT NUMBER(S)

12. DISTRIBUTION/AVAILABILITY STATEMENT
Approved for public release; distribution unlimited

13. SUPPLEMENTARY NOTES
See also ADM002322. Presented at the 2010 IEEE International Radar Conference (9th) Held in Arlington, Virginia on 10-14 May 2010. Sponsored in part by the Navy.

14. ABSTRACT
We present a novel algorithm for radar imaging of point scatterers using a sparse number of spatially separated sensors. Such sparse sensing scenarios are prototypical of many applications wherein a limited number of sensors are distributed over a geographical area; or where environmental and/or systemic constraints enforce a sparse sampling of angular aperture. Our underlying assumption is that the image is sparse with respect to the Gabor basis set. We then introduce the concept of an orbit?viz. the locus of all projections made by a spatial basis?and formulate the radar imaging problem as that of sparsifying the number of orbits that comprise the radon measurements of the source. We demonstrate how our algorithm outperforms FFT-based and Compressive-sensing based reconstruction algorithms for point-scatterer images describe relevant theoretical performance bounds of our algorithm, and point to future research arising from this work.

15. SUBJECT TERMS

16. SECURITY CLASSIFICATION OF:			17. LIMITATION OF ABSTRACT	18. NUMBER OF PAGES	19a. NAME OF RESPONSIBLE PERSON
a. REPORT **unclassified**	b. ABSTRACT **unclassified**	c. THIS PAGE **unclassified**	**Same as Report (SAR)**	**5**	

Given this, the projective signal received at an aspect angle θ_k is: $r_k \equiv R_k I = \mathcal{R}_{\theta_k}\{I\} = \sum_{i=1}^{D} c_i \, \mathcal{R}_{\theta_k}\{\varphi_i(x)\}$ (2)

where, $\mathcal{R}_{\theta_k}$ is the Radon transform taken at aspect angle θ_k. Thus given the data $\{r_k(x)\}_k$, the problem therefore becomes one of inferring the coefficients $\{c_i\}$.

To make our approach concrete, in this paper we employ a Gabor dictionary $\Phi = \{\varphi_i\}_i$ to represent the spatial image. The family of Gabor functions consist of a single prototype function *g(x)* that is modulated by complex exponential: $\varphi_i(x) = g(x)\exp(j\omega_i x)$, where for example *g(x)* is a Gaussian function $g(x) = \frac{1}{\sqrt{2\pi}\sigma_i} exp\left(-\frac{x^2}{2\sigma_i^2}\right)$. A Gabor dictionary is formed by choosing the placement of scale and frequencies, $\{(\sigma_i, \omega_i)\}_i$, of the atoms that constitute the dictionary such that they form a overcomplete basis. In this paper we consider overcomplete Gabor dictionaries with Gaussian prototype windows.

Given a spatial Gabor atom of the form [5-6]:

$$\varphi_i(x) = \frac{1}{\sqrt{\pi\sigma_m\beta_m}} exp\left(-\left[\frac{(x-x_m)^2}{2\sigma_m^2} + \frac{(y-y_m)^2}{2\beta_m^2}\right]\right) \exp\left(j\{\xi_n(x - x_m) + \upsilon_n(y - y_m)\}\right) \quad (1)$$

it can be verified that the Radon projection of (1) is given by:

$$\psi_{k,i}(x) = \mathcal{R}_{\theta_k}\{\varphi_i(x)\} \quad (2)$$

such that:

$$\mathcal{F}\{\varphi_i(x)\}|_{(\xi_n=\omega cos\theta_k, \upsilon_n=\omega sin\theta_k)} = \mathcal{A}\frac{1}{\sqrt{2\pi a_m^2}} \exp\left(-\frac{1}{2a_m^2}(\omega - \omega_m)^2\right) \exp(-j(x_k cos\theta_k + y_k sin\theta_k)\omega) \quad (3)$$

where, $a_m = \sqrt{\sigma_m^2 cos^2\theta_k + \beta_m^2 sin^2\theta_k}$ (4)

$$\omega_m = \left(\frac{\xi_n\sigma_m^2 cos\theta_k + \nu_n\beta_m^2 sin\theta_k}{a_m}\right)^2 \quad (5)$$

$$\mathcal{A} = \sqrt{2\pi a_m^2} exp\left(-\frac{1}{2}(C - d)\right) \quad (6)$$

$$C = \xi_n^2\sigma_m^2 + \upsilon_n^2\beta_m^2 \quad (7)$$

$$d = ((\xi_n\sigma_m^2 cos\theta_k + \nu_n\beta_m^2 sin\theta_k)/a_m)^2 \quad (8)$$

Thus $\psi_{k,i}$ is a Gabor function centered at ω_m with scale a_m and amplitude $\mathcal{A}$. Therefore spatial Gabor atoms project to time-domain Gabor atoms under the Radon transforms. Let us denote the dictionary of time-domain Gabor atoms (that are used to represent the Radon projections) by $\Phi_t = \{\phi_j\}_j$. In the next section we will see how the structure of projections with respect to Φ_t can exploited to estimate the parameters of the spatial Gabor from those of its angular projections.

The above properties together with the fact that Gabors offer a very flexible structure for modeling a range of behaviors from impulses to sinusoids, make Gabor dictionaries good candidates for our applications.

B. The GSAAR Algorithm

Consider a source of *N* point scatterers with positive reflectivities distributed in space and where this source is sensed by *M* sensors equally spaced in a circular geometry. In this paper *M* sensors are assumed to be monostatic and non-interacting. This setup is a prototypical of many scenarios wherein only a limited number of looks are available for a given object in space. Given these sensed measurements, the goal is to reconstruct the image as accurately as possible. The straightforward way to reconstruct this image is to compute the inverse radon transform given the various sensed measurements. In this paper we introduce an alternative algorithm for accomplishing the same objective which we now describe in more detail.

Firstly it is clear that a spatial atom in space projects to various sensing angles when measured by the corresponding sensors. Given this we define an *orbit* of a spatial atom to be the locus of all projections that the atom makes with respect to the various sensing angles. Therefore if an image is sparse in a given dictionary, correspondingly a sparse number of orbits fully account for the *M* radon measurements made with respect to the various sensing angles. The following algorithm infers the orbits that are induced by the spatial atoms that comprise the image:

Greedy Sparse Angular Aperture Radar (GSAAR) Algorithm:

0) $k \leftarrow 1$

1) Compute the optimum pair:

$$(m_k, \psi_k) = \underset{m,\psi}{\text{argmin}} \, | < r_m, \psi > |$$

Let (x_k^0, y_k^0) be the spatial location where atom ψ_k is centered

2) Compute the set

S_k = {*(x,y)*: a Gabor atom centered at *(x,y)* projects to (x_k^0, y_k^0) }

Let $O_k \equiv$ Set of all orbits corresponding to S_k, where the j^{th} orbit corresponds to location (x_k^j, y_k^j) and atoms $\{\phi_{m,k,j}\}_m$ such that:

$$\phi_{m,k,j} = \text{argmin}_{m,\psi} \left| < r_m, \phi^*_{\mathcal{P}_m(x_k^j, y_k^j)} > \right|$$

where:

a) $\phi^*_{\mathcal{P}_i(x_j,y_j)} \in \Phi_t$

b) $\mathcal{P}_m(x_k^j, y_k^j) \equiv$ projection of (x_k^j, y_k^j) onto the m^{th} sensing angle

c) $\phi^*_{\mathcal{P}_m(x_k^j, y_k^j)}$ is the atom that has maximum correlation with r_m among all atoms centered at (x_k^j, y_k^j)

3) Compute the optimum orbit *k* corresponding atoms $\{\phi_m^k\}$ to such that:

$$\{\phi_m^k\} = \underset{j}{\text{argmax}} \, | < \{r_m\}, \{\phi_{m,k,j}\} > |$$

where, $| < \{r_m\}, \{\phi_{m,k,j}\} > | = \sum_{i=1}^{M} | < r_i, \phi_{m,k,j} > |$

4) Estimate the parameters of the spatial atom φ_k corresponding to orbit *k* from the parameters of $\{\phi_m^k\}$

5) Subtract the contribution of orbit *k* from $\{r_m\}$

6) $k \leftarrow k+1$

7) Repeat steps (1-6) until termination criterion is met

The GSAAR algorithm furnishes the spatial bases $\{\varphi_k\}_k$ that comprise the source image. Steps 1-3 of the above algorithm involve identifying the spatial location (x_k, y_k) of the basis φ_k that accounts for the maximum energy in the *M* residual radon measurements. Correspondingly the location of the projections $\{\mathcal{P}_m(x_k, y_k)\}_m$ for each sensing angle θ_m can be determined in a straightforward manner. Let us denote the corresponding optimum atoms centered at $\{\mathcal{P}_m(x_k, y_k)\}_m$ (corresponding respectively to $\{r_m\}_m$) by $\{\phi_m^k\}_m$ (such that $\phi_m^k \epsilon \Phi_t$). Then let $a_{m,k}$ and $\omega_{m,k}$ denote, respectively, the measured scale and center frequency of the Gabor atom ϕ_m^k. First consider measurements of φ_k made at two sensing angles (θ_m, θ_n). Then using equation (4) we obtain the following equation:

$$\begin{bmatrix} \cos^2\theta_m & \sin^2\theta_m \\ \cos^2\theta_n & \sin^2\theta_n \end{bmatrix} \begin{bmatrix} \sigma_k^2 \\ \beta_k^2 \end{bmatrix} = \begin{bmatrix} a_{m,k}^2 \\ a_{n,k}^2 \end{bmatrix} \quad (9)$$

which can be easily solved for (σ_k, β_k). In order to ensure that the matrix in equation (9) is well-conditioned, the angle θ_j can be chosen such that $|\theta_i - \theta_j| \approx \pi/2$. Now given the measured center frequencies $\omega_{m,k}$ and $\omega_{n,k}$, the solution of (9) and equation (5), the center frequency of the spatial Gabor atom can be estimated by solving the following equation:

$$\begin{bmatrix} \sigma_m^2 cos\theta_m & \beta_m^2 sin\theta_m \\ \sigma_n^2 cos\theta_n & \beta_n^2 sin\theta_n \end{bmatrix} \begin{bmatrix} \xi_k \\ \nu_k \end{bmatrix} = \begin{bmatrix} c_{m,k} \\ c_{n,k} \end{bmatrix} \quad (10)$$

where, $c_{m,k} = a_{m,k}\sqrt{\omega_{m,k}}$ and $c_{n,k} = a_{n,k}\sqrt{\omega_{n,k}}$ (11)

Finally the amplitude of the spatial Gabor can be estimated by compensating the amplitude term in (6).

Having estimated the parameters of the spatial atoms above, we then subtract the contributions of this atom from the *M* radon measurements in step (6) of GSAAR. The residual radon measurements are then iteratively analyzed in the same fashion until convergence. Note that convergence to a local minimum is guaranteed since energy of the M radon measurements strictly decreases on every iteration. In the simulations below, since the number of point scatterers is known *a priori*, termination criterion is naturally the number of spatial atoms estimated. Alternatively one can terminate the algorithm once the residual energy falls below a pre-determined threshold.

The next section describes quantitative bounds on the performance of the GSAAR algorithm that gives important insights into some of its theoretical properties.

C. Performance Bounds of the GSAAR Algorithm

A canonical greedy algorithm for approximating the optimum representation of a signal is the OMP (orthogonal matching pursuit) [8]. In this context we demonstrate that the special structure in the greedy approach to sparse angular aperture radar imaging can be easily reduced to a form for which explicit performance bounds have been derived in the literature. The following lemma demonstrates such a reduction.

Lemma 1: Assume that the source image *I* can be exactly represented with respect to all the columns of matrix Φ_{opt}; and let matrix Ψ_{opt} contain the remaining atoms in Φ (and mutually exclusive from Φ_{opt}). Then a sufficient condition for the recovery of $\{r_m\}$ via OMP is as follows:

$$\left\|\widetilde{\Phi}_{opt}^{+}\widetilde{\Psi}_{opt}\right\|_{1,1} < 1 \quad (12)$$

where, $\widetilde{\Phi}_{opt}^{+}$ is the pseudo-inverse of block-diagonal matrix $\widetilde{\Phi}_{opt} = \begin{bmatrix} R_1\Phi_{opt} \\ \vdots \\ R_M\Phi_{opt} \end{bmatrix}$ and $\widetilde{\Psi}_{opt} = \begin{bmatrix} R_1\Psi_{opt} \\ \vdots \\ R_M\Psi_{opt} \end{bmatrix}$.

Proof: The proof follows a similar structure to that of Theorem 3.1 in [8]. Given that is the list of atoms which have been selected until step *k*, let the residual signals, in the k^{th} iteration of the algorithm, be $\{r_i^k\}_i$ where:

$r_i^k \equiv \text{argmin}_a\|r_i - a\|_2$ such that $a \in span\{\phi_\lambda : \lambda \in \Lambda_\lambda\}$

By construction therefore, $r^k = [(r_1^k)^T, \dots, (r_M^k)^T]^T$ is in the column space of $\widetilde{\Phi}_{opt}$: $r^k = \left(\widetilde{\Phi}_{opt}^{+}\right)^* \widetilde{\Phi}_{opt}^* r^k$.

We further observe that a sufficient condition for the OMP to choose another optimum atom is:

$$\rho(r^k) = \frac{\|\Psi_{opt}^* r^k\|_\infty}{\|\widetilde{\Phi}_{opt}^* r^k\|_\infty} < 1 \quad (13)$$

since $\widetilde{\Phi}_{opt}^* r^k$ lists all the inner products of the atoms in $\widetilde{\Phi}_{opt}$ with r^k (and likewise for $\widetilde{\Psi}_{opt}^* r^k$).

But since:

$$\frac{\|\Psi_{opt}^* r^k\|_\infty}{\|\widetilde{\Phi}_{opt}^* r^k\|_\infty} = \frac{\|\Psi_{opt}^* (\Phi_{opt}^+)^* \widetilde{\Phi}_{opt}^* r^k\|_\infty}{\|\widetilde{\Phi}_{opt}^* r^k\|_\infty} < \left\|\widetilde{\Phi}_{opt}^{+}\widetilde{\Psi}_{opt}\right\|_{\infty,\infty} = \left\|\widetilde{\Phi}_{opt}^{+}\widetilde{\Psi}_{opt}\right\|_{1,1}$$

It follows that a sufficient condition for exact recovery of the signal is: $\left\|\widetilde{\Phi}_{opt}^{+}\widetilde{\Psi}_{opt}\right\|_{1,1} < 1$ □

Given the above lemma, the following theorem can be derived [8] which pertains to a general signal not necessarily yielding an exact representation with respect to $\widetilde{\Phi}_{opt}$:

Theorem 1: Assume that $\mu_1(m) < 1/2$ (where, $\mu_1(m) = \max_\psi \sum_{\lambda\in\Lambda_{opt}} \sum_{k=1}^M |\langle\psi, R_k\phi_\lambda\rangle|$, such that Λ_{opt} indexes the atoms in $\widetilde{\Phi}_{opt}$), then OMP recovers an m-term approximation, r^m, of $r = [r_1^T, \dots, r_M^T]^T$ which satisfies:

$$\|r - r_m\|_2 \le \sqrt{1 + C(\widetilde{\Phi}_{opt}, m)}\left\|r - r_{opt}\right\|_2 \quad (14)$$

where, $C(\widetilde{\Phi}_{opt}, m) \le \frac{m(1-\mu_1(m))}{(1-2\mu_1(m))^2}$ □

It can be seen from (13) that the orbit that is chosen by the OMP algorithm corresponds to the atom ϕ for which:

$$\phi = \text{argmax}_\varphi \sum_{i=1}^M |\langle R_i\varphi, r_i\rangle| \quad (15)$$

which is exactly the same criterion used by the GSAAR algorithm (shown in step 3 of the GSAAR algorithm description above). The above analysis applies under the assumption that the coefficients of the atoms selected are obtained via an orthogonal projection to the sub-space spanned by the selected atoms. This of course can be easily incorporated into Step 4 of GSAAR algorithm described in the previous section. In this paper however we have taken a simpler approach of just choosing the coefficient that has the minimum normalized amplitude among all the sensor projections of the chosen orbit. The rationale for such a

simple low-complexity approach is as follows. We say that two spatial atoms collide at θ_m if they have identical quantized projection locations with respect to θ_m (this definition suffices for point scatterers in this paper—but in general will have to be modified also incorporate the scales of the atoms). The ability to resolve *N* spatial atoms therefore hinges on the ability to find sensing angles that separate the pairs of atoms i.e. where collision does not occur. Under the assumption that the source image *I* is infected with zero-mean additive Gaussian noise, we can easily show that the optimal strategy is to average the measurements obtained from the non-collisional projections. However since we do not *a priori* know the collisional structure of the interactions, we conservatively choose the measurement with the minimum value since every projective radon measurement implicitly involves averaging the random fluctuations. This is therefore the strategy that we adopt in this paper.

We further point out that another important factor affecting the performance of the GSAAR algorithm is quantization resolution of the radon measurements made for any given sensing angle—i.e. correspondingly the structure of the dictionary $\widetilde{\Phi} = \left[R_{\theta_1}\{\Phi\}, \ldots, R_{\theta_M}\{\Phi\}\right]$ thus induced. This is partially captured by the coherence condition, $\mu_1(m) < 1/2$, in Theorem 1 which states that optimality of the algorithm can no longer be guaranteed if the mutual coherence between the atoms of the dictionary $\widetilde{\Phi}$ is too high (i.e. if it exceeds 1/2). This mutual coherence condition therefore depends both on the properties of the original image dictionary Φ together with its interaction with the radon transform.

The advantage of GSAAR over a straightforward implementation of OMP is that it has lower computational complexity than the latter because of the fact that the OMP iteratively sifts through all the atoms in the spatial Gabor dictionary until the optimal ones are found due to which all spatial locations must be considered during each iteration of the algorithm. This renders the complexity of OMP for this case to be of the order $O(S)$ where *S* is the number of spatial locations in the source image (and assuming a constant cost of processing for each orbit considered). The GSAAR on the other hand circumvents considering every spatial location by effectively reducing the number of orbits to $O(K\sqrt{S})$, such that $K = O(M)$ (where, *M* is the number of sensors).

III. Simulation Results

Consider *N* point scatterers uniformly distributed in space corrupted by additional Gaussian noise of unit variance and scale factor η. Figure 1 shows a sample distribution of this (without the amplitude information). In the simulations below, this source is sensed by *M*=8 sensors that are uniformly distributed in a circular geometry. The amplitudes of the point scatterers are uniformly distributed in the range [ε, 1] where $\varepsilon > 0$

As explained in Section 2, as a consequence of modeling the spatial image by Gabor atoms, the actual measurements performed by each sensor is a composition of 1-D Gabor functions. Since we are dealing with simple image structures (point scatterers), we construct the Gabor dictionary with scale $\sigma = 0.5$ and with 16 frequency bands whose centers are dyadically placed in a manner similar to the construction of Gabor wavelets in [6].

Table 1 shows the ratio of MSE (mean-square error) in the reconstruction of the source image when GSAAR algorithm as compared to inverse Radon algorithm for varying noise levels. Although we find in all cases that GSAAR outperforms the inverse Radon approach, such a comparison is not entirely fair because it leaves open the possibility that the location of the point scatterers could be inferred from the Fourier reconstructed image by simply choosing the N maximum locations.

Thus in Figure 2 we show, for varying noise levels, the percentage error in detecting the location of the *N* scatterers in space when using the inverse Radon, GSAAR and Compressive Sensing [7] approaches. Figure 3 shows the percentage error for varying number of scatterers but for a fixed noise level. In determining the percentage error for all cases, a non-conflicting spatial location inferred by any algorithm within a radius of ten pixels from a source point scatterer is considered to be a correct inference. In all cases we see that the GSAAR algorithm outperforms both Fourier and Compressive Sensing based approaches when there is even moderate amount of noise present in the system. In these simulations in order to ensure that a maximum operation can in principle retrieve the locations of the *N* point scatterers in space, ε was chosen to be greater than the noise level η. However similar results were obtained for all $\varepsilon > 0$.

These results point to the advantages of imaging in non-Fourier bases and demonstrate how knowledge of the sparse structure of the source images with respect to known dictionaries can potentially be leveraged to obtain superior imaging capabilities over conventional methods of radar imaging.

IV. Discussion

Traditional methods of radar image processing first form the image using Fourier backscattering approach and then analyze the same with respect to various wavelet and overcomplete dictionaries. In this paper we directly form the image from the radon measurements by analyzing the orbital structure of the image. To this end we introduced the GSAAR algorithm wherein the explicit goal is to sparsify the number of orbits that comprise the radon measurements. The special properties of the radon projection of Gabors was utilized to estimate the parameters of the spatial Gabor atoms. The results demonstrate superior performance of the GSAAR algorithm for point scatterer images. The immediate problem arising from this work is that of extending the GSAAR algorithm to handle more complex image structure. Firstly the choice of Gabor dictionary is still likely to be useful although other candidates such as local-cosine bases can also be considered. A related problem is the systematic determination of the multi-scale structure of the source image via the clustering of nearby spatial atoms. These and related issues are the subject of our on-going research efforts.

REFERENCES

[1] D.L. Mensa, High Resolution Radar Cross-section Imaging, 2nd ed, *Artech House*, 1991.

[2] A.K. Jain, Fundamentals of Image Processing, *Prentice Hall*, 1989.

[3] M.A. Richards, Fundamentals of Radar Signal Processing, 1st ed, *McGraw Hill*, 2005.

[4] D.L. Munson, J.D. O'Brien, and W.K. Jenkins, "A Tomographic Formulation of Spotlight-Mode Synthetic Aperture Radar," *Proceedings of the IEEE*, vol. 72, no. 8, February 1983, pp.917-925.

[5] T.S. Lee, "Image Representation using 2-D Gabor Wavelets," *IEEE Transactions on Pattern Analysis and Machine Intelligence*, vol. 18, no. 1O, October 1996, pp. 959-971.

[6] A. C. Bovik, N. Gopal, T. Emmoth, and A. Restrepo, "Localized Measurement of Emergent Image Frequencies using Gabor Wavelets," *IEEE Trans. Information Theory.*, vol. 38, no. 2, March 1992.

[7] E.J. Candès, J. Romberg, and T. Tao, "Robust Uncertainty Principles: Exact Signal Reconstruction From Highly Incomplete Frequency Information," *IEEE Transactions on Information Theory*, vol. 52, no. 2, February 2006, pp. 489-509

[8] J.A. Tropp, "Greed is Good," *IEEE Transactions on Information Theory*, vol. 50, no. 10, 2004, pp. 2231-2242

Noise Levels	0	0.05	0.1	0.15	0.2
MSE_GSAAR/MSE_Fourier	0.2608	0.4033	0.4070	0.4106	0.4116

Table 1: Shows the ratio of the Mean Square Error (MSE) between the GSAAR algorithm and Fourier backprojection methods for varying noise levels and N=25 scatterers. GSAAR consistently gives best MSE performance

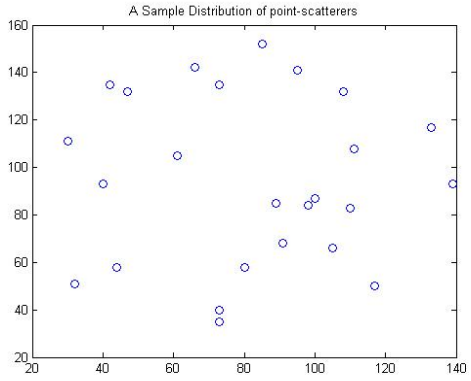

Figure 1

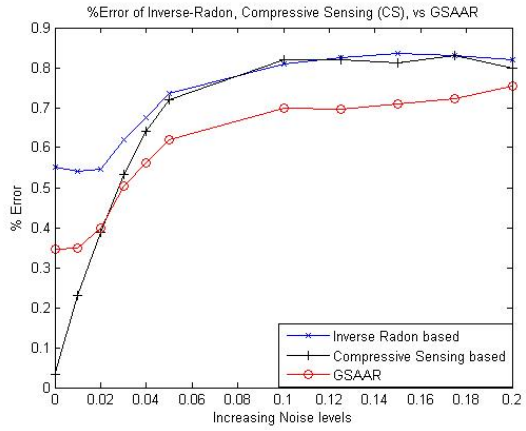

Figure 2

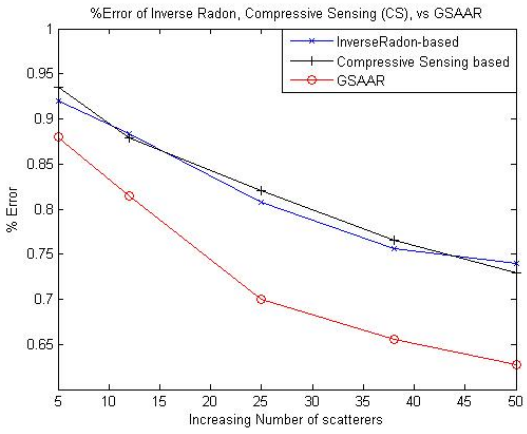

Figure 3

Figure 1: Show a sample distribution of point scatterers

Figure 2: Shows the performance of GSAAR (red; o-), Fourier based (blue; x-) and Compressive sensing based approaches (black; +-) for N=25 scatterers and for varying noise levels

Figure 3: Shows the performance of GSAAR (red; o-), Fourier based (blue; x-) and Compressive sensing based approaches (black; +-) for η=0.1 noise-level and for and for varying number of scatterers